Editors' Suggestion

Cold Active Motion: How Time-Independent Disorder Affects the Motion of Self-Propelled Agents

Fernando Peruani[1] and Igor S. Aranson[2]
[1]Université Côte d'Azur, Laboratoire J.A. Dieudonné, UMR 7351 CNRS, Parc Valrose, F-06108 Nice Cedex 02, France
[2]Materials Science Division, Argonne National Laboratory, Argonne, Illinois 60439, USA
and Department of Biomedical Engineering, Pennsylvania State University, University Park, Pennsylvania, 16802, USA

(Received 26 July 2017; revised manuscript received 18 April 2018; published 6 June 2018)

Assemblages of self-propelled particles, often termed active matter, exhibit collective behavior due to competition between neighbor alignment and noise-induced decoherence. However, very little is known of how the quenched (i.e., time-independent) disorder impacts active motion. Here we report on the effects of quenched disorder on the dynamics of self-propelled point particles. We identified three major types of quenched disorder relevant in the context of active matter: random torque, force, and stress. We demonstrate that even in the absence of external fluctuations ("cold active matter"), quenched disorder results in nontrivial dynamic phases not present in their "hot" counterpart. In particular, by analyzing when the equations of motion exhibit a Hamiltonian structure and when attractors may be present, we identify in which scenarios particle trapping, i.e., the asymptotic convergence of particle trajectories to bounded areas in space ("traps"), can and cannot occur. Our study provides new fundamental insights into active systems realized by self-propelled particles on natural and synthetic disordered substrates.

DOI: 10.1103/PhysRevLett.120.238101

Active matter has become a research topic of broad scientific interest, from soft matter physics to chemistry, biology, and engineering [1,2]. Active self-propelled motion leading to large-scale collective behavior was discovered in living and synthetic systems across scales, from microscopic *in vitro* cytoskeletal extracts [3–5], suspensions of motile bacteria [6,7], motile cell cultures [8,9], colloidal rollers [10–12], and surfers [13], to macroscopic animal herds and bird flocks [14,15]. Theoretical understanding of active matter in terms of nonequilibrium statistical mechanics was achieved by the analysis of discrete particle models (so-called Vicsek-type models) [16,17], phenomenological hydrodynamiclike equations [18,19], or by the asymptotic reduction of the probabilistic Boltzmann equations for particle distribution functions to the Ginzburg-Landau-type equations for the corresponding order parameters [20–22]. Both simulations and the analytic theory led to the overall consensus that the emergence of order is the result of aligning interaction between the neighbors and the misaligning effect of the external noise, e.g., due to thermal fluctuations or bacterial run-and-tumble motion.

External (time-dependent) noise is not the only, and, more importantly, not necessarily the main source of misalignment and disorder in active systems. Self-propelled particles moving on a substrate such as colloidal rollers [10,11], vibrated granular disks [23], gliding myxobacteria [24], etc. can be affected by the substrate imperfection and roughness; flights of birds can be influenced by interfering obstacles or by topographical features. Surfaces with a random pattern of local adhesive strength that affect locomotion of motile eukaryotic cells can be designed, for example, by microcontact printing [25]. Prepatterned surfaces and obstacles, as well as light fields, have already been used in experiments to control and manipulate active particles [26]. Recent experiments with Quincke rollers demonstrated that a random distribution of pinned obstacles can prevent a formation of polar flows, passing through a state where the rollers self-organize their motion into channels [27]. Surprisingly, at a theoretical level still very little is known about how quenched disorder, i.e., time-independent or "frozen" noise, affects the statistical properties of collective motion in active systems. Combining simulations and analytical arguments it has been shown that in the presence of a quenched disorder and a dynamical noise active particles can exhibit subdiffusion [28], and that by increasing quenched disorder, the onset of self-organized polar flows can be suppressed [29,30], as was found experimentally in Ref. [27]. It was also shown that there exists an optimal (dynamical) noise that maximizes collective motion in disordered environments [29,30]. On the other hand, it has been found that volume exclusion can lead to jamming, frozen states, and moving chains [31–34].

In contrast, particle dynamics with quenched disorder is one of the main topics in equilibrium statistical mechanics; it also has enormous practical importance. The motion of Abrikosov vortices in type-II superconductors is the main reason for the dissipation and breakdown of the nonresistive state. Immobilization (or pinning) of the vortices by natural and artificial random defects is the main strategy to fight the dissipation [35]. Pinning of magnetic domains

by defects results in a permanent magnetic moment in ferromagnetic materials [36]. On the other hand, a glassy behavior is typically modeled as the motion of a particle in a random energy landscape [37]. Particle driven in a random potential by an external bias can be described in terms of a "shaking temperature" [38]: moving random pinning landscape generates fluctuations with the overall effect equivalent to a thermal Langevin force. The concept of shaking temperature successfully explained the dynamic melting of the vortex lattice in type-II superconductors [38]. However, the analogy between thermodynamic temperature and the shaking temperature appears to be not complete even in equilibrium systems. Further studies revealed that in contrast to thermal fluctuations, driven vortex lattice flows through well-defined, elastically coupled, static channels [39].

Here, by examining the simplest (or barebone) model of active matter, we investigate the effect of quenched disorder on the motion of self-propelled particles. We identified three main types of spatial disorder termed, correspondingly, random torque (RT), random force (RF), and random stress (RS): RT involves a (local) random turning of the active particle, RF aligns the particle to a local prescribed direction, and RS aligns the particle to a local nematic director; how to implement in practice such disorders are discussed at the end of the Letter. We show that the equations of motion of noninteracting active particles in RT disorder exhibit a Hamiltonian structure, preventing the presence of attractors, and leading to diffusive particle motion. We indicate that by adding particle interactions the system becomes dissipative, making possible the presence of attractors and thus of "particle trapping": i.e., the asymptotic convergence of particle trajectories to bounded areas in space. For RF and RS disorder, there is a lack of Hamiltonian structure for both interacting and noninteracting active particles, and for large disorder strengths particle trapping occurs. In summary, cold active matter is characterized by the presence of a new dynamic phase not present in "hot" system: after a long transient, all particles end up moving in a few closed orbits, i.e., "traps," and the system gets pinned; this new phase is observed at large enough disorder strength for interacting particles in RT disorder, as well as for both noninteracting and interacting particles subject to either RF or RS disorder.

Model.—We consider a continuum-time model for N self-propelled particles moving in a two-dimensional double-periodic domain of size L with quenched disorder. In the absence of particle-particle interactions, the dynamics of the ith active particle is described by

$$\dot{\mathbf{x}}_i = v_0 \mathbf{V}(\theta_i), \qquad \dot{\theta}_i = R_s(\mathbf{x}_i, \theta_i), \tag{1}$$

where the dot denotes temporal derivative, $\mathbf{x}_i$ corresponds to the position of the ith particle, and θ_i is related to its propulsion direction, which is given by $\mathbf{V}(\theta_i) \equiv (\cos(\theta_i), \sin(\theta_i))$, and v_0 is the active speed. The term $R_s(\mathbf{x}_i, \theta_i)$ represents the quenched disorder, with $s = \mathrm{RT}$, RF, RS defined as

$$R_{\mathrm{RT}}(\mathbf{x}_i, \theta_i) = A\Gamma(\mathbf{x}_i), \tag{2}$$

$$R_{\mathrm{RF}}(\mathbf{x}_i, \theta_i) = A \sin\big(\alpha(\mathbf{x}_i) - \theta_i\big), \tag{3}$$

$$R_{\mathrm{RS}}(\mathbf{x}_i, \theta_i) = A \sin\big(2(\alpha(\mathbf{x}_i) - \theta_i)\big), \tag{4}$$

where A is the disorder strength, $\Gamma(\mathbf{x})$ is a random (time-independent) function such that $-1 \le \Gamma(\mathbf{x}) \le 1$, and $\alpha(\mathbf{x})$ is a random (time-independent) phase, with $-\pi \le \alpha(\mathbf{x}) \le \pi$. In order to define the quenched fields $\Gamma(\mathbf{x})$ and $\alpha(\mathbf{x})$, the space is divided into squared cells of size $\Delta_x \times \Delta_x$ in such a way that any point in the space $\mathbf{x}$ has an associated cell. A random value of either Γ or α is assigned to each cell using a uniform distribution in the interval $[-1, 1]$ and $[-\pi, \pi]$, respectively. This implies that $\Gamma(\mathbf{x})$—and similarly for $\alpha(\mathbf{x})$—is such that $\langle \Gamma(\mathbf{x}) \rangle_c = 0$, and $\langle \Gamma(\mathbf{x})\Gamma(\mathbf{x}') \rangle_c = 0$ for $\mathbf{x}$ and $\mathbf{x}'$ belonging to different cells, where $\langle \cdots \rangle_c$ denotes an average taken over all cells. For $\mathbf{x}$ and $\mathbf{x}'$ belonging to the same cell, it reduces to the second moment of the above-defined top-hat distribution, $\langle \Gamma(\mathbf{x})\Gamma(\mathbf{x}') \rangle_c = 1/3$. To account for particle-particle interaction, an extra term I_q can be added to the equations of motion:

$$\dot{\mathbf{x}}_i = v_0 \mathbf{V}(\theta_i), \qquad \dot{\theta}_i = I_q(\mathbf{x}_i, \theta_i) + R_s(\mathbf{x}_i, \theta_i), \tag{5}$$

where $I_q(\mathbf{x}_i, \theta_i)$ represents the interaction of particle i with its neighbors defined by

$$I_q(\mathbf{x}_i, \theta_i) = \frac{1}{n(\mathbf{x}_i)} \sum_{|\mathbf{x}_i - \mathbf{x}_j| < 1} \sin\big(q(\theta_j - \theta_i)\big), \tag{6}$$

where q defines the symmetry of the velocity alignment, with $q = 1$ for polar and $q = 2$ for apolar alignment, and $n(\mathbf{x}_i)$ denotes the number of neighbors of particle i within unit distance. Equations have been nondimensionalized in such a way that the unit of distance corresponds to the radius of interaction and the time unit to the interaction strength. The model defined by Eq. (5) provides a generalization of Vicsek-like models [16] (see also Ref. [40]) with quenched disorder.

Note that due to the Hamiltonian structure of the equations for noninteracting particles with RT disorder and absence of time-dependent noise, see below, simulations have to be performed with a symplectic integrator scheme; see Ref. [41] for details. It is a matter of debate [42,43] on whether the long-time behavior of the discrete-time Vicsek model with dynamic noise depends on the so-called backward [16] and forward update rule [44,45]. Here, we provide solid mathematical arguments that show that for quenched disorder only the forward update rule,

given its symplectic structure, provides a correct description. These arguments, however, cannot be applied to the abovementioned (dynamic noise related) debate.

Results.—Noninteracting particles subject to RT disorder can be mapped to a classical problem of the motion of an electron in a random magnetic field $\Gamma(\mathbf{x})$. To demonstrate that, one takes a time derivative of Eq. (1), for $s = \mathrm{RT}$, that yields after some simple algebra to

$$\ddot{\mathbf{x}} = \dot{\mathbf{x}} \times \big(-A\Gamma(\mathbf{x})\mathbf{z}_0 \big), \tag{7}$$

where $\mathbf{z}_0$ is the unit vector in z directions. In two dimensions, Eq. (7) is a completely integrable system since it has two integrals of motion: the Hamiltonian H and the linear momentum magnitude $|\dot{\mathbf{x}}|^2 = v_0^2$. The Hamiltonian structure of Eq. (7) implies that it cannot have an attractor. Consequently, trajectories cannot converge asymptotically to "preferred areas" of the system, i.e., trapping cannot occur, and particle motion is expected to be diffusive. Numerical simulations confirm that mean squared displacement (MSD) scales linearly with time t, Fig. 1(a). To evaluate the diffusion coefficient of these particles, we employ the concept of shaking temperature T_{sh} [38]. We assume that the disorder strength is small, $A \ll 1$. Since the particle explores the space at a speed v_0, i.e., $\mathbf{x}(t) \approx v_0 t \mathbf{u}_0$, where $\mathbf{u}_0$ is an arbitrary oriented unit vector, we approximate $\theta_i(t) = A\int_0^t dt' \Gamma\big(\mathbf{x}(t')\big) \approx A\int_0^t dt' \Gamma(\mathbf{u}_0 v_0 t')$, assuming that all paths are statistically equivalent. Using the above expression for θ_i, we arrive at

$$\begin{aligned}\langle \theta_i^2(t)\rangle &= 2A^2 \int_0^t dt' \int_0^{t'} dt'' \langle \Gamma(\mathbf{u}_0 v_0 t'')\Gamma(\mathbf{u}_0 v_0 t')\rangle \\ &\approx 2\frac{A^2\langle \Gamma(\mathbf{x})^2\rangle_c \Delta_x}{v_0} t = 2T_{\mathrm{sh}} t. \end{aligned} \tag{8}$$

Thus, similar to thermal systems, the shaking temperature is defined via the disorder correlation $T_{\mathrm{sh}} = A^2\langle\Gamma(\mathbf{x})^2\rangle_c \Delta_x/v_0$. Note that it is required that $\Delta_x > 0$. Thus, we define the angular diffusion coefficient D_θ:

$$D_\theta = T_{\mathrm{sh}} = \frac{A^2\Delta_x}{3v_0}. \tag{9}$$

The corresponding translational diffusion coefficient D_{tr} can be obtained as

$$D_{\mathrm{tr}} = \frac{v_0^2}{2D_\theta} = \frac{3v_0^3}{2A^2\Delta_x}. \tag{10}$$

In contrast to the case of temporal noise where $D_{\mathrm{tr}} \sim v_0^2$, here the diffusion coefficient is proportional to v_0^3. The predictions by Eq. (10) are verified in simulations [41].

Remarkably, the Hamiltonian structure is lost in the interacting case. Interactions formally make the system dissipative. In particular, Eq. (5) for $q = 1$ (polar alignment) can be written in the dissipative Landau-Lifshitz-Gilbert form:

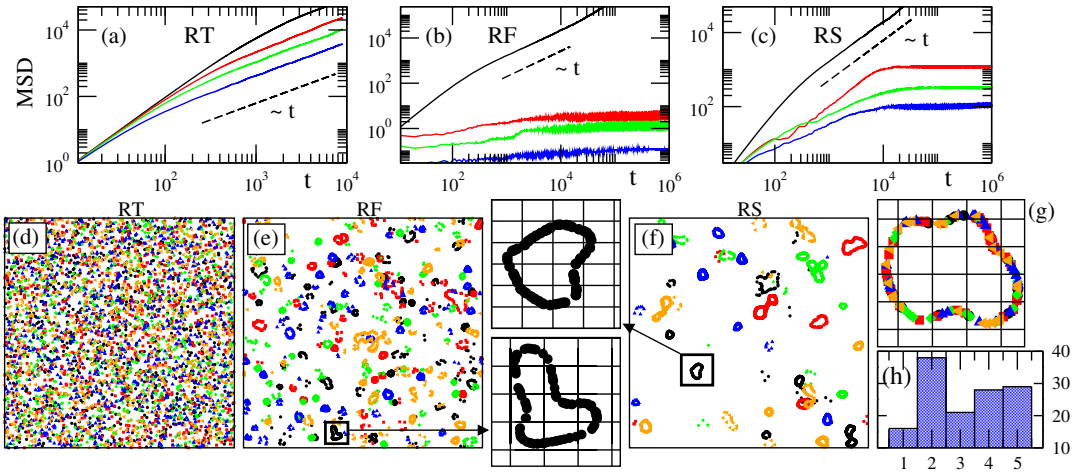

FIG. 1. Noninteracting particles. (a)–(c) Mean squared displacements (MSD) versus time t for RT, RF, and RS disorder, respectively, for different disorder strengths A. The black, red, green, and blue curves correspond to $A = 0.05$, 0.1, 0.3, 0.5 in (a) and $A = 0.1$, 0.5, 1.0, and 5.0 in (b) and (c). (d)–(f) Particle positions for RT, RF, and RS disorder, respectively, at $t = 10^6$ starting from the same initial condition using five different quenched landscapes ($A = 0.5$); particles of the same color move on the same quenched landscape. For RT (d), particle trajectories do not (asymptotically) converge on preferred areas, while for RF and RS, (e) and (f), particles are localized in closed orbits ("traps"): see magnifications of traps in (e) and (f) where each square corresponds to a cell $\Delta_x \times \Delta_x$ containing a time-independent noise value. (g) A trap visited by particles starting from five different random initial conditions (color coded) that moved on the same quenched landscape ($A = 0.5$). (h) The histogram displays the number of particles that landed on the trap shown in (g) from the five different random initial conditions. Parameters are $N = 900$, $L = 30$, $v_0 = 0.1$, and $\Delta_x = 0.5$.

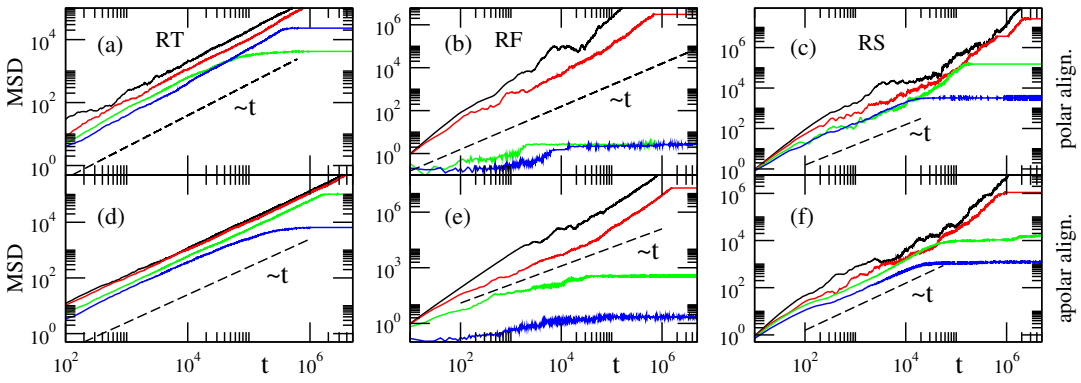

FIG. 2. Interacting particles. MSD versus time t for polar and apolar (velocity) alignment, upper and bottom row, respectively, for RT (a),(d), RF (b),(e), and RS (c),(f) disorder and various disorder strength values A. For movies, see Ref. [41]. Parameters are $N = 900$, $L = 30$, $v_0 = 0.1$, $\Delta_x = 0.5$. The black, red, green, and blue curves correspond to $A = 1.0, 1.5, 2.5, 3.0$ in (a) and (d), $A = 0.005, 0.05, 0.1, 0.3$ in (b), (c), and (e), and $A = 0.1, 0.3, 0.5, 1.0$ in (f).

$$\ddot{\mathbf{x}}_i = -\dot{\mathbf{x}}_i \times A\Gamma(\mathbf{x}_i)\mathbf{z}_0 + \frac{1}{v_0^2 n(\mathbf{x}_i)}\dot{\mathbf{x}}_i \times \sum_{|\mathbf{x}_i-\mathbf{x}_j|<1} \dot{\mathbf{x}}_i \times \dot{\mathbf{x}}_j. \quad (11)$$

This renders possible the presence of attractors and thus the trapping of particles. Numerical simulations confirm that with both polar and apolar interactions, particles asymptotically become localized into traps, as evidenced by the crossover from a diffusive behavior (MSD $\propto t$) to a seemingly saturated value of the MSD; see Figs. 2(a) and 2(d). Note that many timescales may be present: first, the time to find an attractor (crossover from diffusive to saturationlike behavior of MSD) and then a slow (logarithmic) dynamics inside the attractor.

For RF and RS disorder, the equations of motion do not have a Hamiltonian structure, even in the absence of interactions, and thus trapping of particles is possible. In the limit of weak disorder, $A \ll 1$, and for finite time and systems, these two disorders can be approximated to that of RT. To see that, we make an expansion in A for the angle $\theta = \theta_0 + A\theta_1 + A^2\theta_2 + \cdots$. Substituting this expansion into Eq. (1), for $s = \mathrm{RF}$, one obtains $\theta_0 = \mathrm{const}$ and $\dot{\theta}_1 = A \sin(\alpha(\mathbf{x}) - \theta_0) + O(A^2)$. If the angle relation time $\tau = 1/A$ is large compared to the disorder decoherence time $\tau_0 = \Delta_x/v_0$, the problem can be mapped to the RT situation with an effective disorder $\Gamma_{\mathrm{eff}}(\mathbf{x}) = \sin(\alpha(\mathbf{x}))$. Numerical simulations with noninteracting particles in RF and RS disorder confirm that for small values of A normal diffusion is observed, while for large values of A, as expected by the absence of a Hamiltonian structure, particle trapping occurs, Figs. 1(b) and 1(c). Figures 1(e) and 1(f) show some typical examples of traps. From these figures, it is evident that traps are closed orbits found by the active particles that expand over several cells of area $\Delta_x \times \Delta_x$, each of them containing a time-independent noise value.

It is worth mentioning that the system behavior strongly depends on the initial condition and the specific quenched noise landscape that is studied. Figures 1(e) and 1(f) illustrate the sensitivity to quenched noise realization by showing particle positions resulting from five different numerical experiments, all starting with exactly the same initial conditions, and each of them using a different, but statistically identical, quenched disorder landscape. To study the sensitivity to the initial condition, we focus on a single trap (in a given quenched noise landscape) and compute the number of particles that end up in the trap starting from different initial conditions, Fig. 1(h). All this implies that for time-independent disorder there is no unique steady state.

Note that including the interparticle interactions for RF and RS disorder does not restore a Hamiltonian structure and thus attractors may be present and particle trapping possible. Numerical simulations with interacting particles, with either polar or apolar alignment, in RF and RS disorder confirm that particle trapping occurs, Figs. 2(b), 2(c), 2(e) and 2(f). The pinned states (or traps) for interacting particles under RF and RS are similar to those in Figs. 1(e) and 1(f), but with an important difference: interacting particles form high-density clusters that move along the closed orbits (see Ref. [41]). Furthermore, neighboring traps, each of them with a moving cluster, become coupled via the interacting term I_q leading typically to a remarkably slow dynamics where eventually particles fuse and occupy one of the two initial traps, and the behavior of the MSD seems to be (once inside traps) logarithmically slow, i.e., MSD$(t) \propto \log(t)$ (see Ref. [41] for movies and further details).

We indicate that due to quenched noise disorder, long static channels, similar to that predicted for a driven vortex lattice [39], emerge. For finite systems, such long static channels may span the entire system and lead to a (finite-size-related) ballistic regime.

Finally, it is instructive to consider the limiting case of instant alignment with the disorder, corresponding to $A \to \infty$, even if it is out of reach numerically. For $s = \mathrm{RF}$, this limit implies that $\theta = \alpha(\mathbf{x})$ and, thus,

$$\dot{x} = v_0 \cos(\alpha(x,y)), \qquad \dot{y} = v_0 \sin(\alpha(x,y)). \tag{12}$$

The conservation of the magnitude of the linear momentum $|\dot{\mathbf{x}}|^2 = v_0^2$ implies that Eq. (12) cannot have fixed points. On the other had, rigorous topological arguments state that Eq. (12) cannot have periodic orbits either. Indeed, if the disorder function is continuous, then, according to the index theorem [46], in two dimensions any periodic orbit would contain at least one fixed point. Similar considerations apply to the RS disorder. Consequently, in the limit of $A \to \infty$, we expect to recover diffusive behavior.

Concluding remarks.—The presented results can be extended in many directions. While we identified three primary types of disorder (RT, RF, RS), it is likely that in experimental realizations the quenched disorder is not reduced to a specific type but rather a combination of them. Another important aspect is the presence of a time-dependent noise. We anticipate that, depending on the disorder type, time-dependent noise may lead to nontrivial effects, in particular to intermittent trapping of the particles, and thus to the possibility of subdiffusion.

Another intriguing question relates to the limit of $A \gg 1$, in relation to the limiting case given by Eq. (12). The Sinai diffusion model for the motion of a particle in a one-dimensional random potential is a paradigm of glassy dynamics [47]. The model given by Eq. (12) is an interesting generalization of the Sinai diffusion problem to two dimensions. In the limit $\Delta_x \to 0$, Eq. (12) will represent an example of "active glass" and logarithmically slow dynamics at zero temperature. In summary, the limit $A \gg 1$ may unveil interesting new physics.

Finally, depending on the active system in hand, various approaches can be used to engineer a specific disorder type. For example, in bacterial suspensions, the RT disorder can be implemented by varying the hydrodynamic slip length via surface treatment [48,49]; RS can be realized via a random director pattern on a surface, similar to that in Refs. [50–52]. RF can be achieved in the roller system [10,12] via a substrate height modulation.

F. P. was supported by the Agence Nationale de la Recherche via project *BactPhys*, Grant No. ANR-15-CE30-0002-01. I. S. A. was supported by the U.S. Department of Energy, Office of Basic Energy Sciences, Division of Materials Science and Engineering.

[1] T. Vicsek and A. Zafeiris, Phys. Rep. **517**, 71 (2012).
[2] S. Ramaswamy, Annu. Rev. Condens. Matter Phys. **1**, 323 (2010).
[3] T. Sanchez, D. T. Chen, S. J. DeCamp, M. Heymann, and Z. Dogic, Nature (London) **491**, 431 (2012).
[4] Y. Sumino, K. H. Nagai, Y. Shitaka, D. Tanaka, K. Yoshikawa, H. Chaté, and K. Oiwa, Nature (London) **483**, 448 (2012).
[5] V. Schaller, C. Weber, C. Semmrich, E. Frey, and A. R. Bausch, Nature (London) **467**, 73 (2010).
[6] C. Dombrowski, L. Cisneros, S. Chatkaew, R. E. Goldstein, and J. O. Kessler, Phys. Rev. Lett. **93**, 098103 (2004).
[7] A. Sokolov, I. S. Aranson, J. O. Kessler, and R. E. Goldstein, Phys. Rev. Lett. **98**, 158102 (2007).
[8] K. Kawaguchi, R. Kageyama, and M. Sano, Nature (London) **545**, 327 (2017).
[9] T. B. Saw, A. Doostmohammadi, V. Nier, L. Kocgozlu, S. Thampi, Y. Toyama, P. Marcq, C. T. Lim, J. M. Yeomans, and B. Ladoux, Nature (London) **544**, 212 (2017).
[10] A. Bricard, J.-B. Caussin, N. Desreumaux, O. Dauchot, and D. Bartolo, Nature (London) **503**, 95 (2013).
[11] A. Bricard, J.-B. Caussin, D. Das, C. Savoie, V. Chikkadi, K. Shitara, O. Chepizhko, F. Peruani, D. Saintillan, and D. Bartolo, Nat. Commun. **6**, 7470 (2015).
[12] A. Kaiser, A. Snezhko, and I. S. Aranson, Sci. Adv. **3**, e1601469 (2017).
[13] J. Palacci, S. Sacanna, A. P. Steinberg, D. J. Pine, and P. M. Chaikin, Science **339**, 936 (2013).
[14] F. Ginelli, F. Peruani, M.-H. Pillot, H. Chaté, G. Theraulaz, and R. Bon, Proc. Natl. Acad. Sci. U.S.A. **112**, 12729 (2015).
[15] M. Ballerini, N. Cabibbo, R. Candelier, A. Cavagna, E. Cisbani, I. Giardina, V. Lecomte, A. Orlandi, G. Parisi, A. Procaccini *et al.*, Proc. Natl. Acad. Sci. U.S.A. **105**, 1232 (2008).
[16] T. Vicsek, A. Czirók, E. Ben-Jacob, I. Cohen, and O. Shochet, Phys. Rev. Lett. **75**, 1226 (1995).
[17] G. Grégoire and H. Chaté, Phys. Rev. Lett. **92**, 025702 (2004).
[18] J. Toner and Y. Tu, Phys. Rev. Lett. **75**, 4326 (1995).
[19] A. Baskaran and M. C. Marchetti, Phys. Rev. E **77**, 011920 (2008).
[20] I. S. Aranson and L. S. Tsimring, Phys. Rev. E **71**, 050901 (2005).
[21] E. Bertin, M. Droz, and G. Grégoire, Phys. Rev. E **74**, 022101 (2006).
[22] A. Peshkov, I. S. Aranson, E. Bertin, H. Chaté, and F. Ginelli, Phys. Rev. Lett. **109**, 268701 (2012).
[23] J. Deseigne, O. Dauchot, and H. Chaté, Phys. Rev. Lett. **105**, 098001 (2010).
[24] C. W. Harvey, M. Alber, L. S. Tsimring, and I. S. Aranson, New J. Phys. **15**, 035029 (2013).
[25] G. Csucs, K. Quirin, and G. Danuser, Cell Motil. Cytoskeleton **64**, 856 (2007).
[26] C. Bechinger, R. Di Leonardo, H. Löwen, C. Reichhardt, G. Volpe, and G. Volpe, Rev. Mod. Phys. **88**, 045006 (2016).
[27] A. Morin, N. Desreumaux, J.-B. Caussin, and D. Bartolo, Nat. Phys. **13**, 63 (2017).
[28] O. Chepizhko and F. Peruani, Phys. Rev. Lett. **111**, 160604 (2013).
[29] O. Chepizhko, E. G. Altmann, and F. Peruani, Phys. Rev. Lett. **110**, 238101 (2013).
[30] O. Chepizhko and F. Peruani, Eur. Phys. J. Spec. Top. **224**, 1287 (2015).
[31] C. Reichhardt and C. J. Olson Reichhardt, Soft Matter **10**, 7502 (2014).
[32] C. Reichhardt and C. J. Olson Reichhardt, Phys. Rev. E **90**, 012701 (2014).

[33] Y. Yang, D. McDermott, C. J. Olson Reichhardt, and C. Reichhardt, Phys. Rev. E **95**, 042902 (2017).
[34] C. Reichhardt and C. J. O. Reichhardt, arXiv:1803.08992 [Phys. Rev. E (to be published)].
[35] G. Blatter, M. V. Feigel'man, V. B. Geshkenbein, A. I. Larkin, and V. M. Vinokur, Rev. Mod. Phys. **66**, 1125 (1994).
[36] T. Koyama, D. Chiba, K. Ueda, K. Kondou, H. Tanigawa, S. Fukami, T. Suzuki, N. Ohshima, N. Ishiwata, Y. Nakatani *et al.*, Nat. Mater. **10**, 194 (2011).
[37] J.-P. Bouchaud, L. Cugliandolo, J. Kurchan, and M. Mézard, Physica (Amsterdam) **226A**, 243 (1996).
[38] A. E. Koshelev and V. M. Vinokur, Phys. Rev. Lett. **73**, 3580 (1994).
[39] T. Giamarchi and P. Le Doussal, Phys. Rev. Lett. **76**, 3408 (1996).
[40] F. Peruani, A. Deutsch, and M. Bär, Eur. Phys. J. Spec. Top. **157**, 111 (2008).
[41] See Supplemental Material at http://link.aps.org/supplemental/10.1103/PhysRevLett.120.238101, for further technical details and movies.
[42] G. Baglietto and E. V. Albano, Phys. Rev. E **80**, 050103 (2009).
[43] S. Dey, D. Das, and R. Rajesh, Phys. Rev. Lett. **108**, 238001 (2012).
[44] H. Chaté, F. Ginelli, G. Grégoire, and F. Raynaud, Phys. Rev. E **77**, 046113 (2008).
[45] A. P. Solon, H. Chaté, and J. Tailleur, Phys. Rev. Lett. **114**, 068101 (2015).
[46] S. H. Strogatz, *Nonlinear Dynamics and Chaos: With Applications to Physics, Biology, Chemistry, and Engineering* (Westview Press, Boulder, CO, 2014).
[47] Y. G. Sinai, Theory Probab. Appl. **27**, 256 (1983).
[48] J. Hu, A. Wysocki, R. G. Winkler, and G. Gompper, Sci. Rep. **5**, 16329 (2015).
[49] L. Lemelle, J.-F. Palierne, E. Chatre, C. Vaillant, and C. Place, Soft Matter **9**, 9759 (2013).
[50] S. Zhou, A. Sokolov, O. D. Lavrentovich, and I. S. Aranson, Proc. Natl. Acad. Sci. U.S.A. **111**, 1265 (2014).
[51] S. Hernàndez-Navarro, P. Tierno, J. A. Farrera, J. Ignés-Mullol, and F. Sagués, Angew. Chem. **126**, 10872 (2014).
[52] C. Peng, T. Turiv, Y. Guo, Q.-H. Wei, and O. D. Lavrentovich, Science **354**, 882 (2016).